Journal of Sound and Vibration (2000) **231**(2), 411–431
doi:10.1000/jsvi.1999.2722, available online at http://www.idealibrary.com on IDEAL®

THE DYNAMIC RESPONSE OF MULTIPLE PAIRS OF SUBHARMONIC TORSIONAL VIBRATION ABSORBERS

C.-P. CHAO† AND S. W. SHAW

Department of Mechanical Engineering, Michigan State University, East Lansing, MI 48824-1226, *U.S.A.*

(*Received* 15 *September* 1998, *and in final form* 11 *October* 1999)

Recent studies have demonstrated an arrangement of centrifugal pendulum vibration absorbers that is very effective at reducing torsional vibrations in rotating machinery. The basic system is composed of a pair of identical absorbers that are tuned to a one-half subharmonic order relative to the applied fluctuating torque. These absorbers, when moving in an out-of-phase manner along a particular path relative to the rotor, are capable of significantly reducing torsional vibrations of a desired order. In this paper, we consider the response of systems composed of multiple pairs of these absorbers, with the goal of determining the dynamic stability of the desired response and the effects of small imperfections in the absorbers' paths. The desired response of this system is one in which the N absorbers (N even) act as a single pair, with two groups of $N/2$ each moving with equal amplitudes but exactly out of phase with respect to one another. It is shown that this response can be made to be dynamically stable and robust to certain model uncertainties by a slight, identical overtuning of each absorber. The analytical results, obtained by the method of averaging and symmetric bifurcation theory, are confirmed by simulations for the cases with two and three pairs of absorbers.

1. INTRODUCTION

A subharmonic absorber system was proposed by Lee *et al.* [1] for the purpose of reducing torsional vibrations in rotating machinery. The idealized model system consists of a pair of identical masses attached to a rotor in such a manner that they move freely along a prescribed path relative to the rotor. The natural frequency of these absorbers, when the rotor runs at a constant speed, are chosen to be one-half that of the dominant harmonic of the applied torque, and the non-linear parts of their paths have a special form that ensures constant frequency behavior over large amplitudes. It has been shown that this system possesses a dynamically stable response in which the absorbers move (nearly) exactly out of phase with respect to one another in such a manner that they produce a (nearly) perfect harmonic torque

† Currently with Ford Motor Co., Taiwan.

0022-460X/00/120411 + 21 $35.00/0

that can be used to counteract a harmonic torque on the rotor, resulting in a significant reduction in torsional vibration levels.‡ In reference [2] it was shown that this response is quite robust to small system uncertainties, but that a small amount of overtuning can be used to avoid some undesirable response features that may arise from uncertainties in the model.

In practice, one typically needs to choose the total absorber inertia to be sufficiently large such that the absorbers' amplitudes remain below some specified level under the most severe operating conditions. This is typically accomplished by stationing several absorber masses along and around the axis of rotation. These multi-mass arrangements are also used for balancing and/or are due to restricted space around the rotor. In many applications, these absorbers are designed to have identical mass and identical paths. It has been shown that systems of identical absorbers may not always behave in a synchronous manner, and can undergo dynamic bifurcations, resulting in responses that significantly affect performance [3, 4].

In this paper, we consider the dynamic response of a system consisting of a rotor and multiple identical pairs of the subharmonic absorbers, with the goal to determine if it is possible to make them behave as a single absorber pair, and, if so, under what conditions.

Some general features of the equations of motion for an idealized system are first described. They are then massaged by parameter scaling and variable transformations into a form to which averaging can be applied. For simplicity, an asymptotic analysis is first carried out for a system with two pairs of absorbers, in order to predict the stability and potential bifurcations of the desired motion, and the post-bifurcation responses. Under the assumption that all absorber paths are identical and possess an intentional mistuning, the performance of the absorber system is evaluated. This is done by computing two performance measures: the torsional vibration level, as measured by the peak angular acceleration of the rotor during steady state operation, and the range of torques over which the system can effectively operate. Some design guidelines for selecting the absorber paths are distilled from these results. Then, based on analysis and simulations for selected cases, it is shown that these design guidelines are also applicable to cases of several pairs of absorber pairs.

2. THE MULTIPLE SUBHARMONIC ABSORBER SYSTEM

2.1. THE MODEL AND ITS EQUATIONS OF MOTION

The equations of motion are obtained for a system consisting of a rigid rotor spinning about a fixed axis, subjected to an applied torque, and fitted with N (even) point-mass absorbers. The system is shown schematically by the cross-sectional view of the rotor in Figure 1. The rotor has a moment of inertia I_d with respect to the center of rotation, denoted by O, and the N absorbers move along prescribed

‡ Here the term "nearly" is quite precise, since the results are exact in the zero damping limit, and the effects of small damping can be quantified; see references [1, 2].

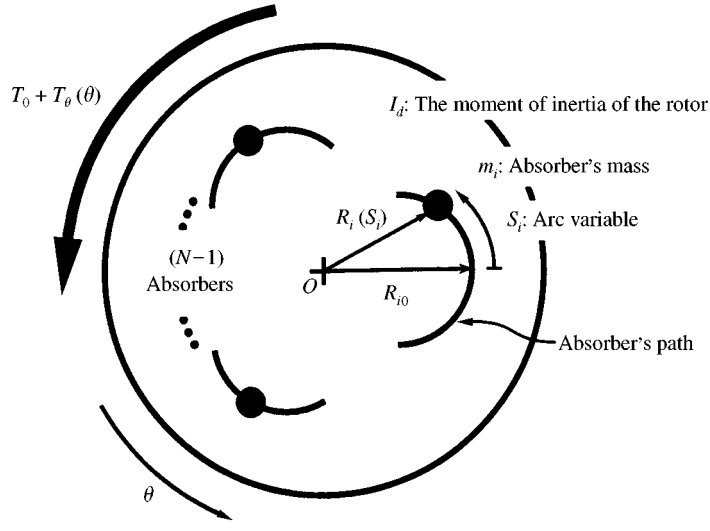

Figure 1. Cross-sectional schematic diagram of the rotor and absorbers.

paths relative to the rotor. The ith absorber is considered to be a point mass with mass m_i.[§] The path for the ith absorber is specified by the function $R_i = R_i(S_i)$, where R_i is the distance from the absorber mass to point O, and S_i is an arc-length variable along the path, defined relative to the rotor. The point $S_i = 0$ is taken to be that at which R_i reaches its maximum value, denoted by $R_{i0} = R_i(0)$. This point is also referred to as the *vertex* of the path. The nominal moment of inertia with respect to O for the ith absorber is defined by $I_i = m_i R_{i0}^2$. The ideal path is designed to be symmetric with respect to its vertex, i.e., $R_i(S_i) = R_i(-S_i)$. The damping between the ith absorber and the rotor is modelled as an equivalent viscous damping with coefficient c_{ai}. Resistance between the rotor and ground is also taken to be an equivalent linear viscous damping with coefficient c_0.

The angle θ denotes the displacement of the rotor. The net applied torque (including load torques) is assumed to be a nominal constant, T_0, plus a disturbing, fluctuating torque $T_\theta(\theta)$, which is periodic in θ. These torques arise from a variety of sources and are generally periodic with several harmonics. They may also depend on $\dot{\theta}$ and $\ddot{\theta}$. For present purposes a single harmonic is taken for the applied torque, as there is typically one dominant harmonic and the absorber system will be designed to suppress torsional vibrations at that order. Therefore, the disturbing torque is assumed to be of order n, $T_\theta(\theta) = \hat{T}_\theta \sin(n\theta)$.

With these assumptions, the overall system kinetic energy can be formulated. Assuming that gravitational effects are small compared to rotational effects and that the corresponding potential energy is negligible, the governing equations of motion are determined by applying Lagrange's method to the kinetic energy. The

[§] It is assumed that the absorbers are suspended in some type of bifilar arrangement [5]. One can account for their moments of inertia about their respective CGs by simply including them in I_d, since they do not rotate with respect to the rotor. However, the rollers often used in such configurations do not follow the rotor, an effect that is considered in reference [6], but not accounted for here.

effects of damping and the applied torque are included by using the appropriate generalized forces. A non-dimensionalization and a change of independent variable are performed on the equations of motion for simplification. To facilitate this process, the nominal steady state rotational speed of the rotor, Ω, is taken to be the speed at which the constant torque T_0 balances the mean component of the torque which arises from rotational damping and load; thus,

$$\Omega = T_0/c_0. \tag{1}$$

Also, a dimensionless variable y, representing the instantaneous rotor speed, is introduced as

$$y \equiv \dot{\theta}/\Omega. \tag{2}$$

Assuming that θ is a smooth and invertible function of t (that is, the rotor never reverses direction), the equations of motion can be transformed into a set of periodically forced, non-autonomous equations with the independent variable θ replacing t. This step transforms the non-linearity, $\hat{T}_\theta \sin(n\theta)$, into a periodic forcing term, and marks the passage of time using the rotor angle in place of t.

The resulting dimensionless dynamical system that describes the dynamics of the N absorbers and the rotor are

$$y s_i'' + [s_i' + g_i(s_i)]y' - \frac{1}{2}\frac{\mathrm{d}x_i}{\mathrm{d}s_i}(s_i)y = -\hat{\mu}_{ai}s_i', \quad 1 \leqslant i \leqslant N, \tag{3a}$$

$$\sum_{i=1}^{N} b_i \left[\frac{\mathrm{d}x_i}{\mathrm{d}s_i} s_i' y^2 + x_i(s_i) y y' + g_i(s_i) s_i' y y' + g_i(s_i) s_i'' y^2 + \frac{\mathrm{d}g_i(s_i)}{\mathrm{d}s_i} s_i'^2 y^2 \right]$$

$$+ y y' = \sum_{i=1}^{N} b_i \hat{\mu}_{ai} g_i(s_i) s_i' y - \hat{\mu}_0 y + \Gamma_0 + \hat{\Gamma}_\theta \sin(n\theta), \tag{3b}$$

where $(\cdot)'$ denotes $\mathrm{d}(\cdot)/\mathrm{d}\theta$, $s_i = S_i/R_{i0}$, $b_i = (m_i R_{i0}^2)/I_d$, $\hat{\mu}_{ai} = c_{ai}/m_i\Omega$, $\hat{\mu}_0 = c_0/I_d\Omega$, $\hat{\Gamma}_0 = T_0/I_d\Omega^2$, $\hat{\Gamma}_\theta = \hat{T}_\theta/I_d\Omega^2$, and

$$x_i(s_i) = \frac{R_i^2(R_{i0}s_i)}{R_{i0}^2} \quad \text{and} \quad g_i(s_i) = \sqrt{x_i(s_i) - \frac{1}{4}\left(\frac{\mathrm{d}x_i}{\mathrm{d}s_i}(s_i)\right)^2} \tag{4}$$

are functions set by the path of the absorber mass. Note that in terms of these dimensionless quantities the steady rotation condition (1) becomes

$$\hat{\Gamma}_0 = \hat{\mu}_0. \tag{5}$$

Also note that there is no restriction on these equations in terms of amplitudes, other than those imposed by physical limitations.

2.2. SYMMETRY PROPERTIES

Here we describe the symmetric nature of the perfectly tuned system, that is, when no imperfections are present. In this case, due to the identical nature of the

absorbers and their paths, it is expected that the system will enjoy some special properties. These properties can be mathematically characterized by transformations among the state variables that yield new sets of system equations which are both structurally and mathematically identical to the original system equations. Such transformations are *symmetries* of the system. Identifying the symmetry of the system allows one to search for and characterize many solutions in an efficient way. To mathematically characterize the symmetries of the system, conventional notation from group theory is employed [7].

To identify the symmetry group of the present model, first consider equation (3), which describes the dynamics of the rotor. It is seen that the speed of the rotor, $y(\theta)$, is invariant under any permutation of the absorbers. Furthermore, from equation (3), it is seen that each absorber is coupled with all other absorbers only through y. Therefore, any permutation of absorbers results in a system that is indistinguishable from the original. Therefore, the symmetry group of the system is $\mathbf{S}_N$, the "symmetric group", containing all permutations on N symbols [8].

Systems with this level of symmetry can be extremely rich in terms of their dynamic behavior. Bifurcations in systems with $\mathbf{S}_N$ symmetry have been studied previously in the context of the dynamics of arrays of Josephson junctions [9]. The high level of symmetry has allowed for some powerful and general results to be obtained regarding the possible bifurcations in these types of systems [9]. Specifically, two basic types of bifurcations can occur. In one type, the full symmetry is maintained through the bifurcation, while in the other type of bifurcating solutions have less symmetry [9]. It is the latter type that is of interest here.

In this system, motions in which groups of absorbers behave in an identical manner will posses multiple eigenvalues. If these become simultaneously unstable, the corresponding bifurcation problem is highly degenerate and there may exist numerous branches of solution emanating from a single bifurcation point. It is not always possible to determine all these branches, let alone their stability types. In the present study, measures of absorber performance are used in conjunction with symmetric bifurcation theory in order to get a handle on the most important branches, and in particular, the dynamically stable ones that define and limit the post-bifurcation, steady state system behavior.

The perfectly tuned system possesses a response in which all absorbers move in perfect unison, thereby behaving as a single absorber; this is labelled the $\mathbf{S}_N$ response, reflecting its level of symmetry. However, for the tuning arrangement proposed, this solution is not dynamically stable (except at very small amplitudes when damping is present). A period-doubling bifurcation occurs at a small torque amplitude, beyond which many steady state solutions are possible. A generic class of post-bifurcation responses has P absorbers moving together (in phase at the same amplitude) while the remaining $N-P$ absorbers move in another self-synchronous group. Such a response is labelled $\mathbf{S}_P \times \mathbf{S}_{N-P}$. Also possible are responses in which there are three groups of absorbers moving together, where one group may even be stationary [9]. The numbers and types of responses depends on the number of absorbers and the system parameter values. Aronson *et al.* [9] have used normal form theory to show that the only stable steady state responses that

can arise from a period-doubling bifurcation in systems with $\mathbf{S}_N$ symmetry are those in which there are two self-synchronous groups of oscillators of roughly equal size. More specifically, stability can occur only for $N/3 \leqslant P \leqslant N/2$. In the present study, the desired response for the absorber system is the $\mathbf{S}_{N/2} \times \mathbf{S}_{N/2}$ response, in which the system of absorbers is dynamically equivalent to a single pair. In this work we shall obtain conditions under which this response can be achieved.

2.3. THE PERFECTLY TUNED ABSORBER SYSTEM

A system consisting of $N/2$ (N even) pairs of identical absorbers with individual masses $m_i = m_0/N$ and identical damping coefficients $\hat{\mu}_{ai} = \hat{\mu}_a$, $i = 1, \ldots, N$, is considered. These absorbers ride on identical paths specified by

$$x_i^2(s_i) = 1 - \left(\frac{n}{2}\right)^2 s_i^2, \quad 1 \leqslant i \leqslant N, \tag{6}$$

which is equivalent to $R_i(S_i) = \sqrt{R_0^2 - (n/2)^2 S_i^2}$. This path is the *tautochronic epicycloid* [6]. These paths tune the non-dimensionalized natural frequency of each absorber to $n/2$, that is, one-half that of the applied torque, and this epicycloid maintains a constant frequency over its entire range of operation—that is, into the large amplitude, non-linear domain.

The equations of motion (3), with the identical paths given by equation (6), have an exact solution when the absorber damping is zero, $\hat{\mu}_a = 0$, and the steady rotation condition (5) is satisfied. This solution represents the $\mathbf{S}_{N/2} \times \mathbf{S}_{N/2}$ response, in which the motions of the absorbers exactly cancel the harmonic applied torque, rendering the rotor speed constant. This mathematical solution is given by

$$y(\theta) = 1, \qquad s_i(\theta) = -\, s_j(\theta) = \pm \frac{2}{n} \sqrt{\frac{2\hat{\Gamma}_\theta}{\nu n}} \cos\left(\frac{n}{2}\theta\right), \tag{7a, 7b}$$

where $i = 1, 3, \ldots, (N-1)$, $j = 2, 4, \ldots, N$ and $\nu = m_0 R_0^2 / I_d$ is the ratio of the total nominal moment inertia of all absorbers about point O to that of the rotor.[¶] The solution described in equation (7) represents a response with a constant rotor speed, exactly as desired.

However, this type of solution is only one of many types that are possible. For example, it is also possible that two of the absorbers move in the desired out-of-phase manner and the other $(N-2)$ remain stationary (an $\mathbf{S}_1 \times \mathbf{S}_1 \times \mathbf{S}_{N-2}$ response). Such a solution is equally valid from a mathematical point of view, although larger absorber amplitudes are required as compared to the case when all absorbers move, thereby resulting in a smaller operating range. Symmetric group theory allows one to completely catalog all such possible steady state responses.

[¶] Note that the subscript labelling is arbitrary; it is only necessary that the absorbers are split into two groups of $N/2$ each. In fact, this implies that the equations of motion have many such solutions.

This is very helpful when trying to determine which responses are even possible, and which of them are dynamically stable.

For a single pair of absorbers ($N = 2$) with small levels of damping, the $\mathbf{S}_2$ synchronous response is dynamically stable for very small torque amplitudes [1]. A period doubling bifurcation occurs as the torque level is increased, rendering the $\mathbf{S}_1 \times \mathbf{S}_1$, out-of-phase, subharmonic response dynamically stable. The angular acceleration of the rotor saturates at a fixed amplitude as the torque level is further increased, up to the point where the absorbers reach cusp points in their epicycloidal paths [1].[††] Both the bifurcation torque and the acceleration saturation level are proportional to the absorber damping magnitude [1]. This response has been shown to be robust to small imperfections in the absorber paths [2].

2.4. IMPERFECTIONS AND LIMITATIONS

The steady state solution in equations (7) corresponds to a perfectly constant rotor speed, which is the ultimate design goal of such an absorber system. In this case, the fluctuating torque is exactly counteracted by the torque induced by the motion of the absorbers. However, absorber damping, imperfections, and other effects render a constant rotor speed unachievable in practice. To account for some of these effects, the absorber path functions are generalized (see reference [2]):

$$x_i(s_i; \hat{\delta}_{ij}) = 1 - \left(\frac{n}{2}\right)^2 s_i^2 - \sum_{j=0}^{Q} \hat{\delta}_{ij} s_i^j, \quad i = 1, 2, \ldots, N, \tag{8}$$

where the $\hat{\delta}_{ij}$'s represent imperfections in the path functions. Note that the $\hat{\delta}_{ij}$'s can incorporate the effects of both intentional mistunings and uncontrolled imperfections. In this work, we focus on intentional mistunings that yield the desired response.

The functions $g_i(s_i)$ must remain real for the absorbers' motions to be physically viable, and this leads to a restriction on their amplitudes—this is the cusp condition. For the case when all imperfections are small, $\hat{\delta}_{ij} \ll 1$, this restriction is approximated by

$$s_i(\theta) \leqslant s_{max} + \mathcal{O}(\hat{\delta}), \quad \forall\theta \text{ and } i \quad \text{where } s_{max} = \frac{4}{n\sqrt{n^2+4}}. \tag{9}$$

The above restriction will impose a finite operating range on the disturbing torque level $\hat{\Gamma}_\theta$, since the amplitudes grow monotonically with the torque level, and the absorbers reach a cusp on the epicycloidal path at this amplitude. A detailed account of this limiting torque is given in reference [2].

[††] An epicycloid can be generated by rolling a circle on the outside of a fixed base circle and tracing out a point that is fixed to the rim of the rolling circle. Such curves have cusp points where they touch the base circle. For an absorber path, such a point is its mathematical limit. In practice, hardware constraints will impose an even smaller limit on the absorber amplitude.

3. REDUCTION OF THE EQUATIONS OF MOTION

In order to evaluate the stability and performance of the absorber system, approximations of the steady state solutions are sought through an asymptotic analysis. We begin with a scaling of the system parameters that brings out the desired behavior. The equations of motion are then expanded in terms of the main scaling parameter, and the equations are rearranged in such a manner that the dynamics of the rotor and the absorbers are separated from one another to leading order. This is followed by two co-ordinate transformations which render the dynamic equations of the absorbers in a standard periodic form which is suitable for the application of averaging.

3.1. PARAMETER SCALING

In applications the total nominal moment of inertia of all absorbers about point O is much smaller than that of the entire rotating system. This motivates the definition of the small parameter,

$$\varepsilon \equiv \nu, \tag{10}$$

which is the ratio of the maximum absorber inertia to the entire rotor inertia. With this definition, the system parameters can be scaled such that the desired features of the system behavior are captured by a first order asymptotic analysis. Hence, it is assumed that the non-dimensional damping and excitation parameters are small and can be scaled as

$$\hat{\mu}_a = \varepsilon\tilde{\mu}_a, \qquad \hat{\mu}_0 = \varepsilon\tilde{\mu}_0, \qquad \hat{\Gamma}_0 = \varepsilon\tilde{\Gamma}_0 \quad \text{and} \quad \hat{\Gamma}_\theta = \varepsilon\tilde{\Gamma}_\theta. \tag{11}$$

These assumptions are realistic for practical problems, since the absorber damping is kept small and the torques are small when scaled by the total kinetic energy of the rotor.

The small imperfections are also scaled by ε,

$$\hat{\delta}_{ij} = \varepsilon\tilde{\delta}_{ij} \quad \forall j \quad \text{and } i = 1, 2. \tag{12}$$

Note that typical values of the $\tilde{\delta}_{ij}$ are less than 1%, whereas ν may range from one to over 10%. The conservative assumption (12) is made in order to incoroporate the effects of imperfections and mistunings in the first order analysis.

The unperturbed system dynamics for this scaling are determined by considering equation (3) with $\varepsilon = 0$, that is, $\nu = 0$, which yields $y = 1$. Using this in equation (3) with $\hat{\mu}_a = 0$ yields a linear oscillator with frequency $n/2$ for each absorber motion. Thus, the steady state solution of the unperturbed system is simply a constant rotor speed, $y = 1$, with the absorbers moving harmonically with frequency $n/2$ and arbitrary amplitudes and phases. This limiting system can be imagined as a very large flywheel attached to the rotor, in which case the absorbers move but have no effect on the rotor.

Since the rotor speed will change smoothly as the absorber mass, the applied torque and the absorber damping are increased from zero, y will be smooth in ε and can be expanded as

$$y(\theta) = 1 + \varepsilon y_1(\theta) + \mathcal{O}(\varepsilon^2), \tag{13}$$

where y_1 captures the leading order speed fluctuations induced by the net interaction of the applied torque, damping effects, and the torques induced by the movements of the absorbers. Note that condition (5) is assumed to maintain as ε is increased from zero, thereby keeping the mean rotational rate near $y = 1$.

3.2. THE ROTOR ANGULAR ACCELARATION

It is convenient to have an explicit expression for the rotor angular acceleration, since it is a measure of the torsional vibration amplitude of the rotor. With the scaling employed, it is clear that the rotor will run at nearly constant speed and, therefore, the angular acceleration, $yy'(= \ddot{\theta})$, will be small. Starting with equation (3), one can obtain a leading order approximation for yy' by making use of the path function definitions given in equations (4) and (8), the scaling defined in the previous section, and the conditions given in equation (5). The result is found to be

$$yy'(\theta) = \varepsilon\left\{\frac{1}{N}\sum_{j=1}^{N}\left(\frac{n^2}{2}s_j s_j' - g^0(s_j)s_j - \frac{\mathrm{d}g^0(s_j)}{\mathrm{d}s_j}s_j'^2\right) + \tilde{\Gamma}_\theta \sin(n\theta)\right) + \mathcal{O}(\varepsilon^2), \tag{14}$$

where

$$g^0(s_i) = g_i(s_i; \hat{\delta}_{ij} = 0) = \sqrt{1 - \left(\frac{4n^2 + n^2}{16}\right)s_i^2}, \quad i = 1, \ldots, N.$$

The above equation expresses the rotor acceleration in terms of the dynamics of the absorbers. The fact that the non-dimensionalized angular acceleration is of order ε is consistent with the limiting case as $\varepsilon \to 0$. A detailed study of how the peak value of the steady state acceleration depends on the system parameters can be found in reference [2]. Also note that y' is equal to yy' to leading order. Therefore, by considering equation (13) it is seen that the function $y_1(\theta)$ can be determined in terms of the absorber dynamics through equation (14).

3.3. THE ABSORBER DYNAMICS

It is possible to obtain a set of equations of motion in which the dynamics of the N absorbers are uncoupled from the rotor dynamics to leading order. This is accomplished by starting with equation (3) and dividing it through by y (since y is never zero). Then, one uses equation (13) to recognize that y'/y is the same as yy' to leading order. Next, utilizing equations (13) and (14), the path definitions, the scaling conditions, and expanding the result in terms of ε, a set of weakly coupled, weakly non-linear oscillators for the absorber dynamics is obtained. These

oscillators, in which the dynamics of the rotor has been eliminated to first order, are given by

$$s_i'' + \left(\frac{n}{2}\right)^2 s_i = \varepsilon f_i(\mathbf{s}, \mathbf{s}', \theta) + \mathcal{O}(\varepsilon^2), \quad i = 1, \ldots, N, \tag{15}$$

where

$$f_i(\mathbf{s}, \mathbf{s}', \theta) = -\tilde{\mu}_a s_i' - h_i(s_i) + [s_i' + g^0(s_i)]\left[\frac{1}{N}\sum_{j=1}^{N}\left(-\frac{n^2}{2}s_j s_j' - \left(\frac{n}{2}\right)^2 g^0(s_j)s_j + \frac{\mathrm{d}g^0(s_j)}{\mathrm{d}s_j}s_j'^2\right) - \tilde{\Gamma}_\theta \sin(n\theta)\right],$$

$$h_i(s_i) = \frac{1}{2}\sum_{k=1}^{Q} k\tilde{\delta}_{ik} s_i^{k-1},$$

and $\mathbf{s}$ is simply the vector with s_i as elements.

Remarks

- The unperturbed frequencies of these absorber oscillators are identical. Thus, there exists a $1:1 \ldots 1:1$ internal resonance in the absorber dynamics.
- The excitation is in a $2:1$ resonance with respect to each absorber, and it is of both external and parametric form.
- Any imperfections that are distinct among the absorbers destroy the embedding symmetry of the system, that is, the $\mathbf{S}_N$ disappears.

3.4. THE PERIODIC STANDARD FORM

These oscillator equations (15) are now put into the standard periodic form by using two co-ordinate transformations. The first is the following linear co-ordinate transformation among absorber displacements:

$$\xi_1 = \frac{1}{N}\sum_{j=1}^{N} s_j, \quad \xi_i = \frac{1}{N}(s_1 - s_i) \quad \text{for } 2 \leqslant i \leqslant N, \tag{16}$$

which splits the dynamics into two invariant subspaces, one representing the synchronous motion and the other its complement. The second transformation is to polar co-ordinates, representing the amplitudes and phases of these modes:

$$\xi_i = r_i \cos\left(\varphi_i - \frac{n\theta}{2}\right), \qquad \xi_i' = r_i \frac{n}{2}\sin\left(\varphi_i - \frac{n\theta}{2}\right), \quad \text{for } 1 \leqslant i \leqslant N. \tag{17}$$

Implementing the transformations in equations (16) and (17) transforms equations (15) into the standard periodic form given by,

$$r_i' = \varepsilon\frac{2}{n}\hat{F}_i(r_1, \ldots, r_N, \varphi_1, \ldots, \varphi_N, \theta)\sin\left(\varphi_i - \frac{n\theta}{2}\right) + \mathcal{O}(\varepsilon^2), \tag{18a}$$

$$r_i\varphi_i' = \varepsilon\frac{2}{n}\hat{F}_i(\tau_1, \ldots, r_N, \varphi_1, \ldots, \varphi_N, \theta)\cos\left(\varphi_i - \frac{n\theta}{2}\right) + \mathcal{O}(\varepsilon^2), \tag{18b}$$

where $1 \leqslant i \leqslant N$, and the functions $\hat{F}_i$ result from incoporating transformations (16) and (17) in the f_i, $1 \leqslant i \leqslant N$, given in equations (15). Note that the first mode, (r_1, φ_1), represents a response in which all absorbers move in perfect unison. If the remaining modes are zero, the response is purely unison. Non-unison components are captured by the modes (r_i, φ_i) for $i = 2, \ldots, N$.

4. THE AVERAGED EQUATIONS

Considering only the leading order terms in ε in equations (18), first order averaging is performed over one period of excitation, $4\pi/n$. The resulting averaged equations can be expressed in terms of the first order averaged variables, $\bar{r}_i$, and $\bar{\varphi}_i$, $1 \leqslant i \leqslant N$. Due to the complicated nature of the f_i's in equation (15), the averaging process does not yield closed-form expressions for each term in the averaged equations. To circumvent this problem, two assumptions are made. First, the oscillation amplitudes of absorbers, that is, $\bar{r}_i$ $1 \leqslant i \leqslant N$, are assumed to be small and of the same order, denoted by $\mathcal{O}(\bar{r})$. The resulting averaged equations are then expanded in terms of $\bar{r}_i$, $1 \leqslant i \leqslant N$ up to $\mathcal{O}(\bar{r}^3)$ (the first non-linear order terms) in order to capture the resonant, post-bifurcation solutions. Second, it is assumed that the relative precision between the curves for the absorber paths is much higher than their absolute precision, which renders nearly identical absorber paths. This can be arranged in practice by imposing intentional imperfections that dominate any uncertainties in the path. It is therefore assumed that the imperfection parameters scale as

$$\frac{\tilde{\sigma}_{ij}}{\tilde{\sigma}_{1j}} = \mathcal{O}(\varepsilon) \quad \text{for } 2 \leqslant i \leqslant N, \quad j = 1, 2, \ldots, \tag{19}$$

where

$$\tilde{\sigma}_{1j} = \frac{1}{N} \sum_{i=1}^{4} \tilde{\delta}_{ij}, \quad j = 1, 2, \ldots, Q,$$

$$\tilde{\sigma}_{ij} = \frac{1}{N} (\tilde{\delta}_{1j} - \tilde{\delta}_{ij}), \quad 2 \leqslant i \leqslant N, \quad j = 1, 2, \ldots, Q.$$

These steps result in a set of averaged equations of the form

$$\frac{\mathrm{d}\bar{r}_1}{\mathrm{d}\hat{\theta}} = {}^{-}\!\!\!\!\frac{1}{2}\,\tilde{\mu}_a \bar{r}_1 + \tfrac{1}{4}\tilde{\Gamma}_\theta \bar{r}_1 \sin 2\bar{\varphi}_1 + \hat{G}_1(r_1, \ldots, r_N, \varphi_1, \ldots, \varphi_N) + \mathcal{O}(\bar{r}^5), \tag{20a}$$

$$\bar{r}_1 \frac{\mathrm{d}\bar{\varphi}_1}{\mathrm{d}\hat{\theta}} = \left(-\frac{\tilde{\sigma}_{12}}{n} - \frac{n}{2} \right) \bar{r}_1 + \frac{1}{4}\tilde{\Gamma}_\theta \bar{r}_1 \cos 2\bar{\varphi}_1 + \hat{H}_1(r_1, \ldots, r_N, \varphi_1, \ldots, \varphi_N) + \mathcal{O}(\bar{r}^5), \tag{20b}$$

$$\frac{d\bar{r}_i}{d\hat{\theta}} = \tfrac{1}{2}\tilde{\mu}_a \bar{r}_i + \tfrac{1}{4}\tilde{\Gamma}_\theta \bar{\Gamma}_i \sin 2\bar{\varphi}_i + \hat{G}_i(r_1, \ldots, r_N, \varphi_1, \ldots, \varphi_N) + \mathcal{O}(\bar{r}^5), \tag{20c}$$

$$\bar{r}_i \frac{d\bar{\varphi}_i}{d\hat{\theta}} = -\frac{\bar{\sigma}_{12}}{n}\bar{r}_i + \frac{1}{4}\tilde{\Gamma}_\theta \bar{r}_i \cos 2\bar{\varphi}_i + \hat{H}_i(r_1, \ldots, r_N, \varphi_1, \ldots, \varphi_N) + \mathcal{O}(\bar{r}^5), \tag{20d}$$

where $2 \leqslant i \leqslant N$, $\hat{\theta} \equiv \varepsilon\theta$, and the $\hat{G}$ and $\hat{H}$ functions contain the $\mathcal{O}(\bar{r}^3)$ terms resulting from averaging. Due to the complexity of these functions and their dependence on the number of absorbers, they are not listed explicitly here. However, it is not difficult to obtain them by following the procedure described.

Note that with scaling assumption (19), which dictates nearly identical absorber paths, the averaged equations (20) still possesses the isotropy subgroup $\mathbf{S}_N$ up to $\mathcal{O}(\bar{r}^3)$. It is also seen that a level of internal mistuning between the modes is evident in these averaged equations through the presence of the term $-n\bar{r}_1/4$ in equation (20b). This will be shown to be a key factor in predicting the post-bifurcation responses of the system.

5. CASE STUDIES

Results for systems with two pairs of subharmonic absorbers ($N = 4$) are presented in detail. The averaged equations are analyzed to determine the steady state solution branches and their corresponding stabilities. A similar analysis was carried out for systems with three pairs of absorbers, but the details are not shown here. Based on the results obtained for $N = 2, 4, 6$, some general conclusions are drawn. It is found that for a system with $N/2$ pairs of absorbers, only the solutions with isotropy subgroups $\mathbf{S}_{N/2} \times \mathbf{S}_{N/2}$ and $\mathbf{S}_1 \times \mathbf{S}_{N-1}$ are viable as stable and feasible solutions that do not violate the peak amplitude condition. Furthermore, it is found that one can avoid the $\mathbf{S}_1 \times \mathbf{S}_{N-1}$ response by proper selection of the mistuning parameters, thereby insuring that the desired response is achieved. These results have been confirmed by numerical simulations of the original equations of motion for $N = 2, 4, 6$.

5.1. TWO PAIRS OF ABSORBERS: STEADY STATE SOLUTION BRANCHES

Steady state solutions are determined by the stationary points of the averaged equations. These can be categorized by their symmetry properties. Once the solutions have been determined, the corresponding stability types are determined by evaluating the corresponding Jacobians of the averaged equations.

It is difficult to determine all solution branches due to the high level of symmetry and the dimension of the system's averaged equations (20). However, the restriction on the absorber motions described in equations (9) imposes an upper limit on the

feasible torque range. This condition facilitates the search for the steady state solution branches of interest.

It can be shown by evaluating the Jacobian of equations (20) that, for small values of $\bar{\sigma}_{12}$, the trivial solution (which represents the S_N response) becomes unstable as $\tilde{\Gamma}_\theta$ approaches $2\tilde{\mu}_a$; thus, $\tilde{\Gamma}_\theta^* \simeq 2\tilde{\mu}_a$ where $\tilde{\Gamma}_\theta^*$ denotes the critical torque level at the first bifurcation point. This agrees with the known result for a single absorber pair [1]. Based on the structure of equations (20a) and (20b), one can show that $\bar{r}_1 \simeq 0$ and $\tilde{\Gamma}_\theta \to (2\tilde{\mu}_a)^+$, due to the effect of the internal mistuning. In the following, $\bar{r}_1 \simeq 0$ will be applied to determine the post-bifurcation responses.

In the post-bifurcation stage, the system might converge to any steady state solution with non-zero components of $\bar{r}_i$, $2 \leqslant i \leqslant 4$. To classify these solutions, the following sets of indices are defined:

$$\hat{\mathscr{Z}} \equiv \left\{ i \,|\, \lim_{\theta \to \infty} \bar{r}_i(\theta) = 0,\ 2 \leqslant i \leqslant 4 \right\}, \qquad \hat{\mathscr{N}} \equiv \left\{ i \,|\, \lim_{\theta \to \infty} \bar{r}_i(\theta) \neq 0,\ 2 \leqslant i \leqslant 4 \right\}, \quad (21)$$

which are sets of integers containing those indices corresponding to zero and non-zero steady state amplitudes, respectively. For those $\bar{r}_i$ with $i \in \hat{\mathscr{Z}}$, the solution for the steady state phase $\bar{\varphi}_i$ is arbitrary. For the remaining $\bar{r}_i$'s, that is, those with $i \in \hat{\mathscr{N}}$, it can be assumed that the corresponding phases are identical, i.e., $\bar{\varphi}_i = \bar{\varphi}_j$, $\forall i, j \in \hat{\mathscr{N}}$ (see reference [4] for a justifying argument for a similar problem). Applying these results and $\bar{r}_1 \simeq 0$ to equations (20c) and (20d) yields the result that the post-bifurcation solutions must satisfy the equations

$$0 = \tfrac{-1}{2}\tilde{\mu}_a + \tfrac{1}{4}\tilde{\Gamma}_\theta \sin 2\bar{\varphi}, \quad (22a)$$

$$0 = \frac{-\tilde{\sigma}_{12}}{n} + \frac{1}{4}\tilde{\Gamma}_\theta \cos 2\bar{\varphi} - \frac{1}{32n}\Psi(\bar{r}_i; \bar{r}_2, \bar{r}_3, \bar{r}_4, \tilde{\sigma}_{14}), \quad i \in \hat{\mathscr{N}}, \quad (22b)$$

where

$$\bar{\varphi} = \bar{\varphi}_i, \quad i \in \hat{\mathscr{N}}, \quad (23a)$$

$$\begin{aligned}\Psi(\bar{r}_i; \bar{r}_2, \bar{r}_3, \bar{r}_4, \bar{\sigma}_{14}) = {} & 3n^4\bar{r}_2^2 + 3n^4\bar{r}_3^2 + 3n^4\bar{r}_4^2 - 2n^4\bar{r}_2\bar{r}_3 - 2n^4\bar{r}_3\bar{r}_4 - 2n^4\bar{r}_2\bar{r}_4 \\ & + 192\tilde{\sigma}_{14}(4\bar{r}_i^2 - 3\bar{r}_2\bar{r}_i - 3\bar{r}_3\bar{r}_i - 3\bar{r}_4\bar{r}_i) \\ & + 144\tilde{\sigma}_{14}(\bar{r}_2^2 + \bar{r}_3^2 + \bar{r}_4^2 + 2\bar{r}_2\bar{r}_3 + 2\bar{r}_2\bar{r}_4 + 2\bar{r}_3\bar{r}_4).\end{aligned} \quad (23b)$$

Equations (22) lead to

$$\Psi(\bar{r}_i; \bar{r}_2, \bar{r}_3, \bar{r}_4, \bar{\sigma}_{14}) = \Psi(\bar{r}_j; \bar{r}_2, \bar{r}_3, \bar{r}_4, \bar{\sigma}_{14}), \quad i, j \in \hat{\mathscr{N}}, \quad (24)$$

a required condition for a non-synchronous, steady state response.

Note that equation (24) is automatically satisfied for a system with zero fourth order imperfections (that is, $\bar{\sigma}_{14} = 0$) due to the invariance of the function $\Psi(\bar{r}_i; \bar{r}_2, \bar{r}_3, \bar{r}_4, 0)$ under arbitrary exchange of $[\bar{r}_2, \bar{r}_3, \bar{r}_4]$. In this case, there exist an infinite number of steady state solutions (at this level of approximation) which lie on an ellipsoid prescribed by

$$\mathscr{E}^0 = \{[\bar{r}_2, \bar{r}_3, \bar{r}_4] \,|\, \Phi(\bar{r}_i; \bar{r}_2, \bar{r}_3, \bar{r}_4, 0) = 0\}, \tag{25}$$

where

$$\Phi(\bar{r}_i; \bar{r}_2, \bar{r}_3, \bar{r}_4, \tilde{\sigma}_{14}) = -32\tilde{\sigma}_{12} + 8n(\tilde{\Gamma}_\theta^2 - 4\tilde{\mu}_a^2)^{1/2} - \Psi(\bar{r}_i; \bar{r}_2, \bar{r}_3, \bar{r}_4, \tilde{\sigma}_{14}). \tag{26}$$

However, in practice, the fourth order imperfection $\tilde{\sigma}_{14}$ is a small, non-zero quantity, and its presence will select out specific solutions on the ellipsoid. This fact, and its geometrical interpretation, is used to help determine the possible steady state solutions that satisfy equations (22).

The ith components of equations (22) are satisfied for any solutions lying on the ellipsoid

$$\mathscr{E}^i = \{[\bar{r}_2, \bar{r}_3, \bar{r}_4] \,|\, \Phi(\bar{r}_i; \bar{r}_2, \bar{r}_3, \bar{r}_4, \tilde{\sigma}_{14}) = 0\} \tag{27}$$

and the steady state solution of the overall system must simultaneously satisfy equations (22) for all $i \in \hat{\mathscr{N}}$. Hence, the possible steady state solutions lie on the intersection points of the $\mathscr{E}^i$ for $i \in \hat{\mathscr{N}}$. That is, the set

$$\mathscr{S} = \bigcap_{i \in \hat{\mathscr{N}}} \mathscr{E}^i \tag{28}$$

contains all possible steady state solutions. Figure 2 depicts the graphical relationship among these ellipsoids, where the case with $\hat{\mathscr{N}} = \{2, 3\}$ is shown. It is seen from this figure that with a small, non-zero $\tilde{\sigma}_{14}$, each ellipsoid $\mathscr{E}^i$ is slightly distorted away from $\mathscr{E}^0$, but in a different preferred direction for different i. This results in a finite number of steady state solutions, which lie at the four intersection points, denoted by I_j, $1 \leqslant j \leqslant 4$, in the figure.

Based on equations (27) and (28), the intersection points, that is, the steady state solutions, can be found be solving

$$\Phi(\bar{r}_i; \bar{r}_2, \bar{r}_3, \bar{r}_4, \tilde{\sigma}_{14}) = \Phi(\bar{r}_j; \bar{r}_2, \bar{r}_3, \bar{r}_4, \tilde{\sigma}_{14}) = 0, \quad i, j \in \hat{\mathscr{N}}, \tag{29}$$

which automatically satisfies equation (24).

All solutions in the set $\mathscr{S}$ can be classified by examining equation (24). They are listed in Table 1, where the corresponding isotropy subgroup is used for the classification. It is seen from this table that there exist only three distinct types of solutions: $\mathbf{S}_2 \times \mathbf{S}_2, \mathbf{S}_1 \times \mathbf{S}_3, \mathbf{S}_1 \times \mathbf{S}_1 \times \mathbf{S}_2$. Note that the existence of two different mode shapes for the $\mathbf{S}_1 \times \mathbf{S}_3$ and $\mathbf{S}_1 \times \mathbf{S}_1 \times \mathbf{S}_2$ solution branches is simply due to different choices of s_1. In fact, they are dynamically equivalent since the absorbers

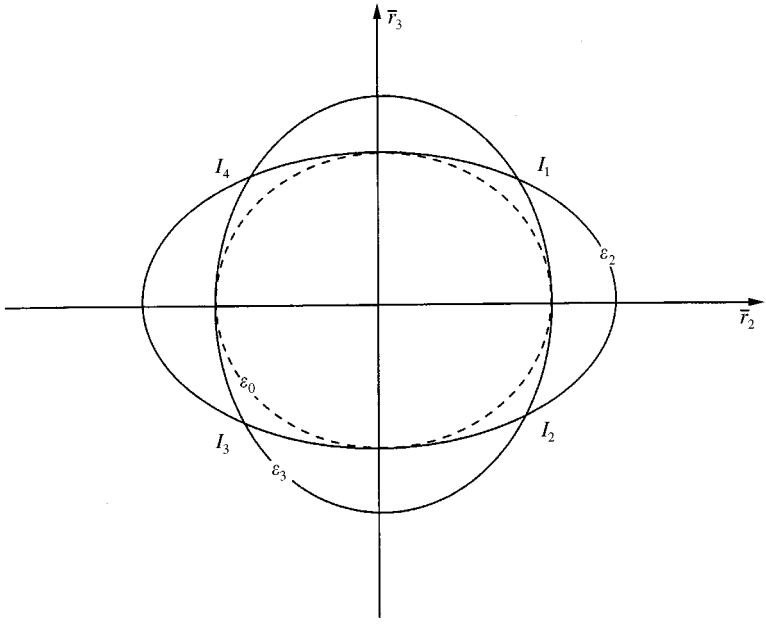

Figure 2. A graphical representation of the distorted ellipsoids.

TABLE 1

The solutions branches classified by their isotropy subgroups and their mode shapes

Isotropy subgroup	Mode shapes of $[\bar{r}_2, \bar{r}_3, \bar{r}_4]$
$\mathbf{S}_2 \times \mathbf{S}_2$	$[\bar{r}, \bar{r}, 0]$
$\mathbf{S}_1 \times \mathbf{S}_3$	$[\bar{r}, \bar{r}, \bar{r}]$ or $[\bar{r}, 0, 0]$
$\mathbf{S}_1 \times \mathbf{S}_1 \times \mathbf{S}_2$	$[\bar{r}, -\bar{r}, 0]$ ir $[\bar{r}, \bar{r}, 2\bar{r}]$

are essentially indistinguishable. Figure 3 depicts the typical time responses for these three solution types.

With these possibilities in hand, the steady state solutions can be obtained by solving equations (29). Then, by numerically evaluating the Jacobian of the truncated, averaged equations (20) at these solutions, one can determine the corresponding stability types for each steady state solution.

5.2. ABSORBER PERFORMANCE AND DESIGN GUIDELINES

The absorber performance is evaluated by computing the two performance measures, torsional vibration amplitude and operating torque range, based on the solution branches and their stabilities. However, due to the high multiplicity of the post-bifurcation solutions and the complexity of the corresponding stability boundaries, closed-form representations of the two performance measures are not

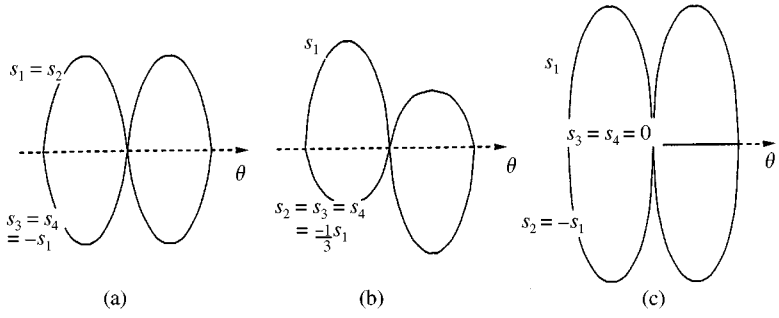

Figure 3. The mode shapes of the steady state solutions with various isotropy groups (a) $\mathbf{S}_2 \times \mathbf{S}_2$; (b) $\mathbf{S}_1 \times \mathbf{S}_3$; (c) $\mathbf{S}_1 \times \mathbf{S}_1 \times \mathbf{S}_2$.

pursued. The design guidelines are based on results and general trends obtained from a case study using specific parameter values, with the imperfections considered as design variables.

The common system parameters used for this study are $\hat{\Gamma}_\theta = 0{\cdot}035$, $\hat{\mu}_a = 0{\cdot}005$, $n = 2$ and $\nu = 0.1662$.‡‡ The stability and feasibility boundaries for the three different forms of the steady state solutions were investigated as functions of the two imperfection parameters, $\hat{\sigma}_{12}$ and $\hat{\sigma}_{14}$ ($\hat{\sigma}_{12}$ and $\hat{\sigma}_{14}$ denote the unscaled versions of $\tilde{\sigma}_{12}$ and $\tilde{\sigma}_{14}$. i.e., $\hat{\sigma}_{ij} = \varepsilon\tilde{\sigma}_{ij}$). Figures 4 and 5 show the stability and feasibility boundaries for two of these responses. In these figures, "S" and "U" denote stable and unstable regions, respectively, and the dashed line divides the feasible and infeasible regions, dictated by whether or not any of the corresponding absorber motions reach their cusps. It is seen that among these two types of solutions, large sets of the $\mathbf{S}_2 \times \mathbf{S}_2$ and the $\mathbf{S}_1 \times \mathbf{S}_3$ solutions survive as stable and feasible. A similar diagram for the $\mathbf{S}_1 \times \mathbf{S}_1 \times \mathbf{S}_2$ solutions indicates that only a very tiny set of parameters, similar to the set in area "abc" in Figure 5, are stable and feasible. The responses in these small regions are not considered since the absorbers are almost certain to hit the cusps in transition to the steady state.

It is clear that one can insure that the system behaves in the desired manner if both of the imperfection parameters are taken to be positive, rendering the $\mathbf{S}_2 \times \mathbf{S}_2$ response stable, the $\mathbf{S}_1 \times \mathbf{S}_3$ response unstable, and the $\mathbf{S}_1 \times \mathbf{S}_1 \times \mathbf{S}_2$ unfeasible at moderate torque levels. Taking both mistuning parameters as negative also yields the desired solution as stable and feasible, and renders the other solutions unfeasible. However, this case is not as desirable because, as is seen subsequently, torsional vibration levels are larger in this parameter range.

The absorber performance is now quantified in the larger of the stable "S" regions for the two types of solutions under consideration. Figure 6 shows the contours of the rotor acceleration for a fixed torque level, $\hat{\Gamma}_\theta = 0{\cdot}035$, for the stable and feasible solutions in the "S" regions. It is seen that the positive mistuning range offers better vibration reduction than the negative mistuning range.

‡‡ The latter parameters are taken from 2·5 l, in-line, four-stroke, four cylinder engine considered by Denman [6].

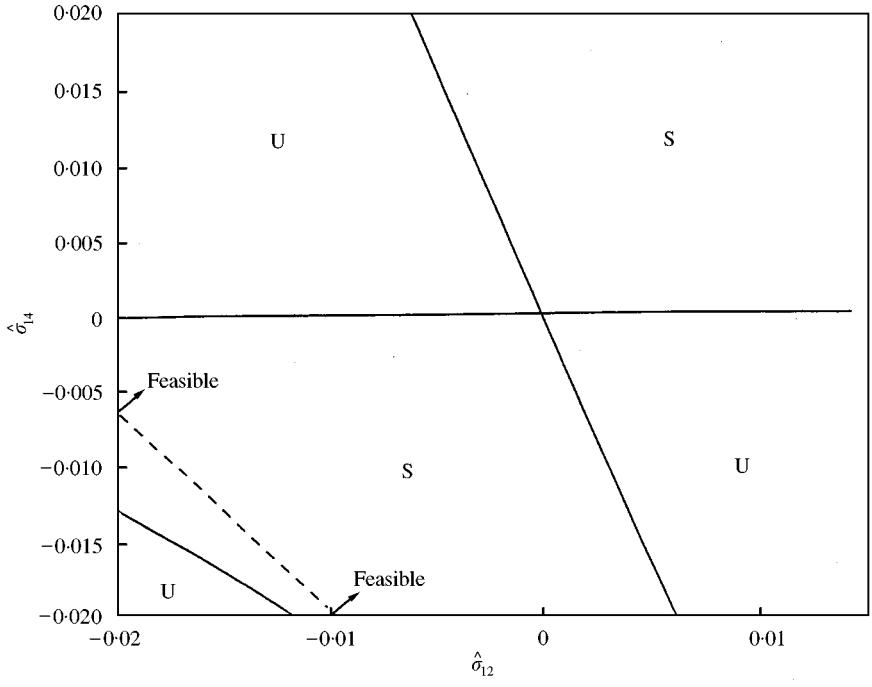

Figure 4. The stability and feasibility boundaries of the solutions with isotropy subgroup $\mathbf{S}_2 \times \mathbf{S}_2$ for the case study.

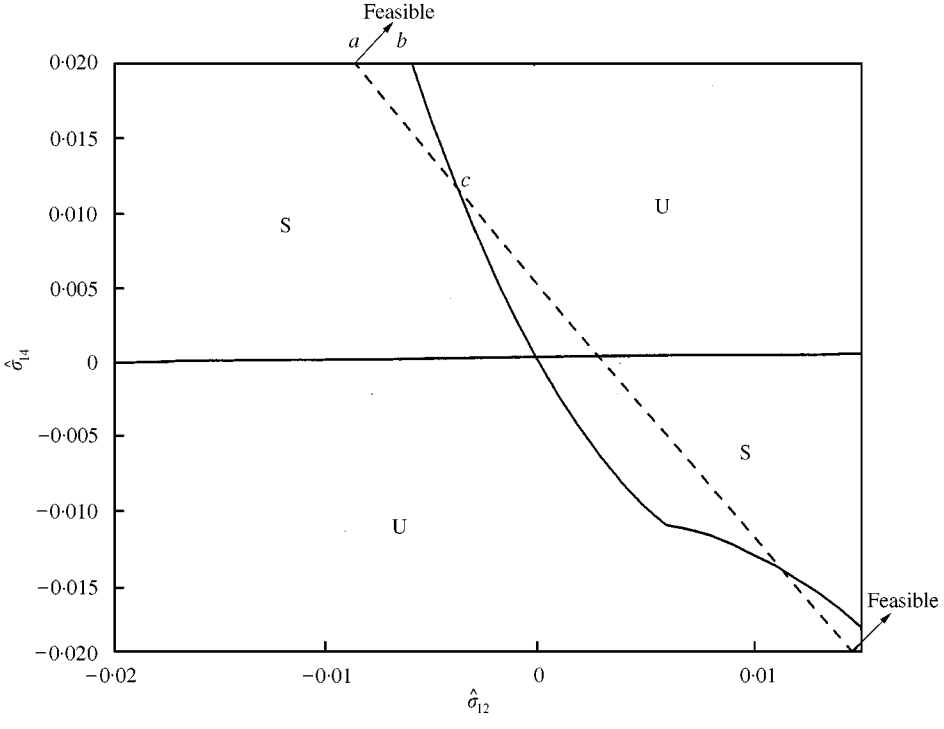

Figure 5. The stability and feasibility boundaries of the solutions with isotropy subgroup $\mathbf{S}_1 \times \mathbf{S}_3$ for the case study.

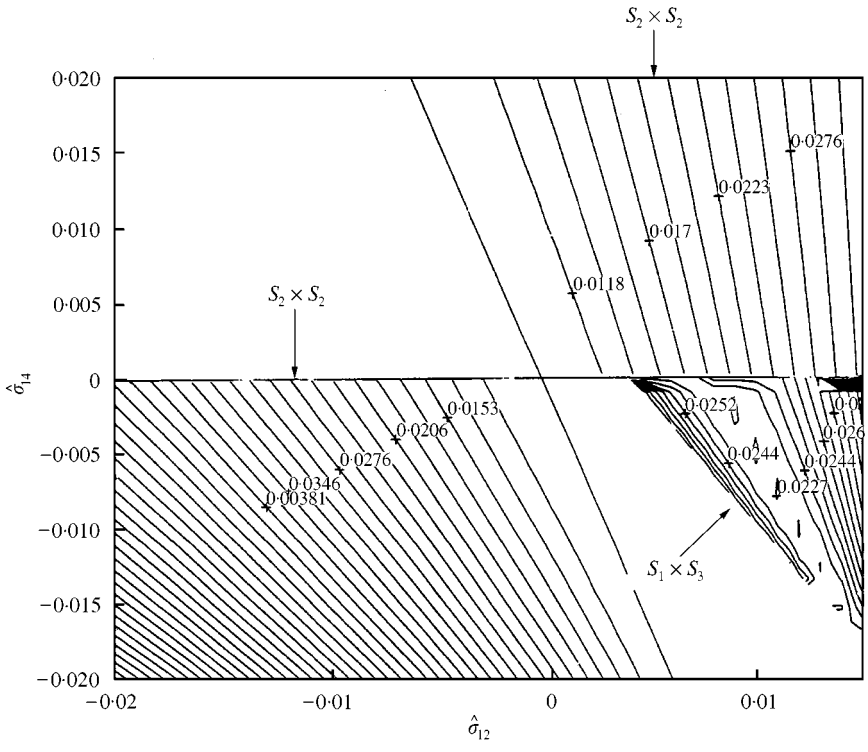

Figure 6. The contours of the rotor accelerations for $\hat{\Gamma}_\theta = 0{\cdot}035$, $\hat{\mu}_a = 0{\cdot}005$, $n = 2$ and $\nu = 0{\cdot}1662$.

By using the expression for the rotor acceleration in equation (14) and the limitation on absorber motions given in inequality (9), one can compute the feasible torque operating range. Figure 7 shows the feasible ranges of the disturbing torque for the $\mathbf{S}_2 \times \mathbf{S}_2$ solution branch as a function of the mistuning parameters. It is observed that one can extend the operating range by moving further into the positive mistuning range, but at the expense of performance, cf. Figure 6.

It is seen from Figures 6 and 7 that small, positive values of the $\hat{\sigma}_{12}$'s and $\hat{\sigma}_{14}$'s leads to a stable $\mathbf{S}_2 \times \mathbf{S}_2$ response and achieves a good balance between a small rotor accelerations and a large feasible torque range, exactly as desired.

A thorough set of numerical simulations, based on the fully non-linear original equations of motion, confirmed the validity of these predictions.

5.3. ARBITRARY PAIRS OF ABSORBERS

A similar analysis can be conducted for a system with an arbitrary number (N even) of absorbers. The following conclusions are drawn from the results described in reference [2] for one pair of absorbers, those described above for two pairs of absorbers, and from a study of the system with three pairs of absorbers, the details of which are not presented here.

- As the number of absorbers increases, the number of possible solution branches increases, and these can be classified by their symmetry groups. For example,

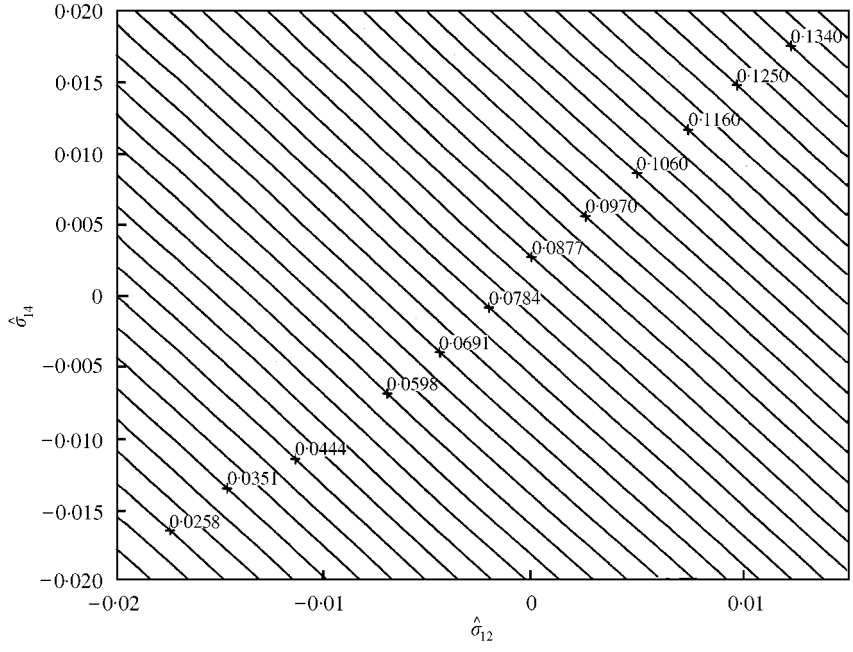

Figure 7. The operating torque range of the $\mathbf{S}_2 \times \mathbf{S}_2$ solution branch for $\hat{\mu}_a = 0{\cdot}005$, $n = 2$ and $v = 0{\cdot}1662$.

there exist five distinct types of steady state solution branches for $N = 6$. This fact significantly complicates the analysis. However, it was found that only the solutions with isotropy subgroups $\mathbf{S}_{N/2} \times \mathbf{S}_{N/2}$ and $\mathbf{S}_1 \times \mathbf{S}_{N-1}$ are stable and feasible solutions (in terms of not coming close to or violating the cusp conditions).

- Small differences in the paths, described in the model by small non-zero values of $\hat{\sigma}_{ij}$, $2 \leqslant i \leqslant N$, lead to a decrease in the operating torque range and an increase of the rotor acceleration (both undesirable), while non-symmetric and higher order imperfections (corresponding to $\hat{\sigma}_{ij}, j = 1, 3, 5, 6, \ldots$) do not have a significant effect on the system performance.
- The dependence of the absorber performance on the imperfection parameters $\hat{\sigma}_{12}$ and $\hat{\sigma}_{14}$ is similar to that found for $N = 4$. Positive, small $\hat{\sigma}_{12}$ and $\hat{\sigma}_{14}$ render a stable $\mathbf{S}_{N/2} \times \mathbf{S}_{N/2}$ response, and lead to smaller rotor accelerations over an acceptable torque range.

6. SUMMARY

In summary, the results obtained in this study dictate that the following general guidelines be followed when designing the paths for systems of subharmonic absorbers:

- The absorber paths should be kept as identical as possible.
- The parameters $\hat{\sigma}_{12}$ and $\hat{\sigma}_{14}$, which represent linear and non-linear mistuning of the tautochronic epicycloidal absorber path, should be selected to be small and

positive. Their values should be sufficient to overcome any imperfections that may arise due to wear, thermal effects, or other types of distortion. This can be accomplished by design of the mechanisms by which the absorber masses are suspended.

- One can make tradeoffs between performance, in terms of torsional vibration levels and the torque operating range, by varying the magnitudes of the imperfection parameters $\hat{\sigma}_{12}$ and $\hat{\sigma}_{14}$.

ACKNOWLEDGMENTS

This work has been supported by a grant from the National Science Foundation.

REFERENCES

1. C.-T. Lee, S. W. Shaw and V. T. Coppola 1997 *ASME Journal of Vibration and Acoustics* **119**, 590–595. A subharmonic vibration absorber for rotating machinery.
2. C-P. Chao and S. W. Shaw 1998 *Journal of Sound and Vibration* **215**, 1065–1099. The effects of imperfections on the performance of the subharmonic vibration absorber system.
3. C.-P. Chao, S. W. Shaw and C.-T. Lee 1997 *ASME Journal of Applied Mechanics* **64**, 149–156. Stability of the unison response for a rotating system with multiple centrifugal pendulum vibration absorbers.
4. C.-P. Chao, C.-T. Lee and S. W. Shaw 1997 *Journal of Sound and Vibration* **204**, 769–794. Non-unison dynamics of multiple centrifugal pendulum vibration absorbers.
5. W. Ker Wilson 1968 *Practical Solution of Torsional Vibration Problems*. Vol. IV. London: Chapman & Hall Ltd, chapter XXX, third edition.
6. H. H. Denman 1992 *Journal of Sound and Vibration* **159**, 251–277. Tautochronic bifilar pendulum torsion absorbers for reciprocating engines.
7. M. Golubitsky, I. Stewart and D. G. Schaeffer 1988 *Singularities and Groups in Bifurcation Theory*, Vol. II. New York: Springer-Verlag.
8. D. S. Dummit and R. M. Foote 1991 *Abstract Algebra*. Englwood Cliffs, NJ: Prentice-Hall.
9. D. G. Aronson, M. Golubitsky and M. Krupa (1991) *Nonlinearity* **4**, 861–902. Coupled arrays of Josephson junctions and bifurcation of maps with S_N symmetry.
10. A. K. Bajaj, P. Davies and S. I. Chang 1995 On internal resonances in mechanical systems. *Nonlinear Dynamics and Stochastic Mechanics* (W. Kliemann and N. Sri Namachchivaya, editors) 69–94. Boca Raton: CRC press.
11. V. J. Borowski, H. H. Denman, D. L. Cronin, S. W. Shaw, J. P. Hanisko, L. T. Brooks, D. A. Milulec, W. B. Crum and M. P. Anderson 1991 *SEA Technical Paper Series* 911876. Reducing vibration of reciprocating engines with crankshaft pendulum vibration absorbers.
12. S. L. Chen and S. W. Shaw 1996 *International Journal of Bifurcation and Chaos* **6**, 1575–1578. A fast-manifold approach to melnikov functions for slowly-varying oscillators.
13. D. L. Cronin 1992 *Mechanism and Machine Theory* **27**, 517–533. Shake reduction in an automobile engine by means of crankshaft-mounted pendulums.
14. J. P. Den Hartog 1938 *Stephen Timoshenko* 60*th Anniversary Volume*, 17–26. New York: The Macmillan Company. Tuned pendulums as torsional vibration eliminators.
15. H. H. Denman 1985 *American Journal of Physics* **53**, 781–782. Remarks on brachistochrone-tautochrone problems.
16. E. Doedel 1985 *Auto: Software for continuation and bifurcation problems in ordinary differential equations*. Department of Applied Mathematics, California Institute of Technology, Pasadena, CA.

17. C.-T. Lee and S. W. Shaw 1994 *Nonlinear and Stochastic Dynamics*, *ASME*, *WAM*, volume 7 ADM-Vol. 192/DE-Vol. 78, 91–98. A comparative study of nonlinear centrifugal pendulum vibration absorbers.
18. C.-T. Lee and S. W. Shaw 1997 *Journal of Sound and Vibration* **203**, 731–743. Nonlinear dynamic response of paired centrifugal pendulum vibration absorbers.
19. J. F. Madden 1980 *United States Patent No.* 4218187. Constant frequency bifilar vibration absorber.
20. J. A. Murdock 1991 *Perturbations*: *Theory and Methods*. New York: John Wiley & Sons.
21. D. E. Newland 1964 *ASME Journal of Engineering for Industry* **86**, 257–263. Nonlinear aspects of the performance of centrifugal pendulum vibration absorbers.
22. S. W. Shaw, V. K. Garg and C.-P. Chao 1997 *SAE Noise and Vibration Conference and Exposition*, Attenuation of engine torsional vibrations using tuned pendulum absorbers, Vol. 2, 713–722. *The Society of Automotive Engineers*.
23. S. W. Shaw and C.-T. Lee 1995 *Smart Structures*, *Nonlinear Vibrations*, *and Control* (A. Guran and D. J. Inman, editors) 247–309 New Jersey: Prentice-Hall Inc., On the nonlinear dynamics of centrifugal pendulum vibration absorbers.